Natural Convection Inside a Horizontal Cylinder

WILLIAM R. MARTINI and STUART W. CHURCHILL

The University of Michigan, Ann Arbor, Michigan

The two vertical halves of the wall of a 4.3-in. I.D. cylinder were maintained at different uniform temperatures. The rate of circulation of air inside the cylinder and the local rate of heat transfer between the wall and air were derived from measurements of the velocity and temperature fields in the air for wall-temperature differences from 3.5° to 367°F. The over-all rate of circulation was found to increase quite rapidly and then to decrease slowly as the wall-temperature difference was increased. The over-all Nusselt number based on the wall-temperature difference was found to have an approximately constant value of 7.0.

Numerical solution of the partial differential equations describing the conservation of mass, momentum, and energy for this system was investigated with an IBM-650 magnetic drum computer. Instabilities in the computational procedure and limitations of this computer prevented solution of the general problem. However specification of the velocity field obtained from experiment yielded a numerical solution for the temperature field in good agreement with the experimental measurements.

The importance of natural convection in space heating and meteorology has long been recognized. More recently attention has been given to such applications as the emergency cooling of nuclear reactors, the cooling of gas turbine blades, and the recombination of the oxygen and hydrogen involved in water-boiler types of nuclear reactors. Nevertheless natural convection, particularly in enclosed spaces, has been a relatively neglected field of investigation.

Apparently natural convection in a horizontal cylinder has been studied experimentally only by Ostroumov (*1*), who discussed the determination of the temperature gradients in glycerine by an optical method but did not present any data. Zhukhovitskii and others (*2, 3, 4*) outlined a method for the approximate solution of the mass, energy, and momentum equations describing natural convection. Results in agreement with the unpublished experimental work of Ostroumov were claimed. The method appears to be applicable only for low temperature differences and/or for fluids of high viscosity, and only for very special boundary conditions.

In this investigation a long horizontal circular cylinder and a step function in temperature at the vertical diameter were chosen for simplicity. Since the primary purpose was to provide insight into the transfer processes, the temperature and velocity fields were measured rather than the heat flux at the wall.

Numerical solution of the partial differential equations for describing the conservation of mass, energy, and momentum in this system was investigated with an electronic digital computer. The possibilities of this technique are discussed and the computed values compared with the measured values.

Only representative data, final correlations, and conclusions are presented in this article. The complete data and additional details are included in reference (*5*).

EXPERIMENTAL APPARATUS

Figure 1 is a diagram of the experimental apparatus. A 3-ft. length of 4-in. standard iron pipe was cut in two lengthwise and welded into two iron jackets as shown. The inside surface of the pipe was machined to a uniform diameter of 4.3 in., and the two boxes were then positioned with a cylindrical template. A ¼- by 3-in. channel was constructed completely through one jacket, and a Lucite window was fitted in the pipe wall at the end of this channel to permit illumination of the inside of the pipe. The ends of the pipe were closed with glass plates.

The ½-in. space between the jackets above and below the pipe was filled with asbestos felt. With the exception of the windows, the jackets were covered with 4 in. of insulation and a layer of aluminum foil. A plug of insulation covered the Lucite window when it was not in use for velocity measurements.

Heat was supplied to one jacket by electrical resistance elements. The energy input was regulated by a variable transformer and measured by a wattmeter. The jacket was filled to a depth of 2 or 3 in. with acetone water, Dowtherm A or Dowtherm E and evacuated to remove air from the vapor space. A condenser was mounted in the top of the jacket so that the entire jacket was filled with vapor or liquid at the saturation temperature. The pressure was measured with a mercury manometer, which also served as a safety valve.

The other jacket was filled almost to the top with acetone. Originally it had been planned to allow the acetone to boil and then to condense on the cooling coils, but operation with the cooling coils immersed in the liquid yielded a more uniform wall temperature. To minimize leaks, a slight vacuum was maintained on the cooling jacket. The rate of heat removal through the cooling coils in the two jackets was determined by passing the cooling water through rotameters and measuring the inlet and outlet temperatures.

TEMPERATURE MEASUREMENT

Cooling water and wall temperatures were measured with calibrated, 30-gauge, copper-constantan thermocouples. Fourteen thermocouples located at various points in the cylinder wall indicated that longitudinal temperature gradients were negligible in the central half of the cylinder wall. Consequently a two-dimensional temperature and velocity field was assumed to exist in the air in the central region. The reported temperatures of the hot and cold wall were measured in thermowells that penetrated almost to the inside surface at the horizontal diameter. Thermocouples soldered to the outside of the walls at the top and bottom indicated that the temperature variation

William R. Martini is with Atomics International, Canoga Park, California.

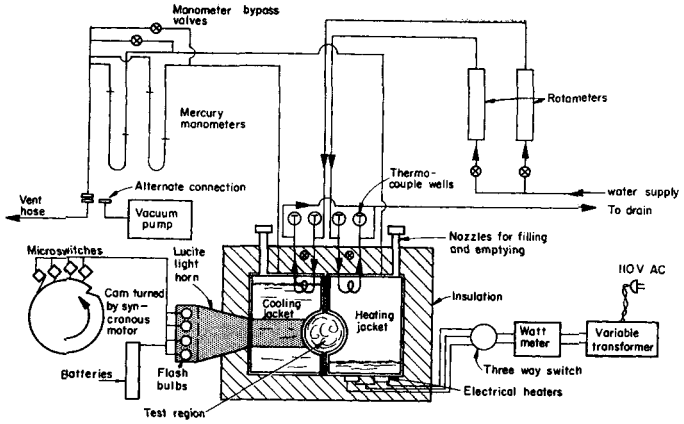

Fig. 1. Diagram of experimental apparatus.

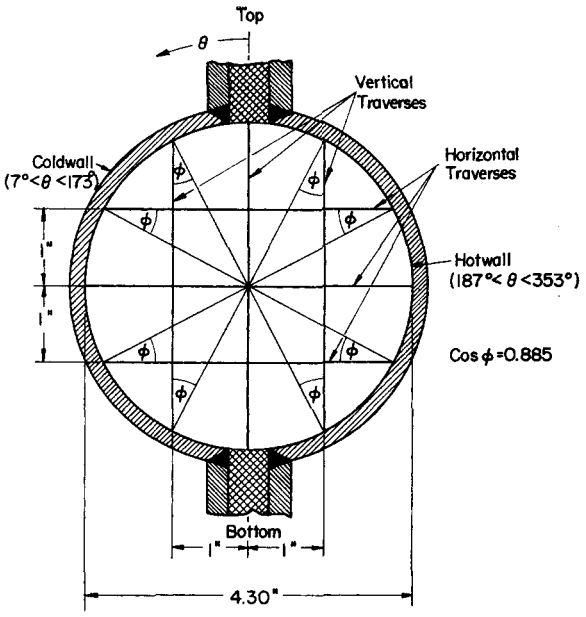

Fig. 2. Experimental geometry.

over the walls was less than 10% of the temperature differences between the walls. The experimental boundary condition thus closely approached the idealized case of a step function in wall temperature.

The air temperature was measured with a calibrated, 40-gauge, chromel P–alumel thermocouple stretched parallel to the axis of the cylinder with the junction at the center. This single wire was supported by a rod across each end of the cylinder, just inside the glass end plates. A small spring at one end of the wire maintained tension. The two rods were allowed to slide in three horizontal and three vertical grooves. The location of the temperature traverses is indicated in Figure 2. To position the thermocouple, the rods were placed in corresponding grooves at the two ends; then each rod was moved by hand until the stretched wire was aligned with grid lines on the end plates. Energy balances for the 40-gauge thermocouple wires indicate that the effect of radiation on the air-temperature measurements and on the desired heat transfer rates was negligible.

VELOCITY MEASUREMENT

The velocity field was determined by photographing dust particles suspended in the air. A small quantity of titanium-dioxide pigment having particle diameters from 3 to 7 μ was blown into the center of the test space through a small tube. The flow pattern reestablished itself in about 30 sec. after introduction of the dust. The settling velocity of the particles was calculated to be 0.05 to 0.2 in./sec., which was negligible compared with the air velocity in most of the region.

The particles were illuminated through the Lucite window in one side of the cylinder. Fast-peaking flash bulbs were used so that the flow measurements would be completed before the flow could be affected by the thermal radiation. The time scale of the acceleration due to the bulbs was observed to be far greater than the period of exposure. A Lucite light horn directed the light from the bulbs into the center of the test regions as indicated in Figure 1. The bulbs were fired by microswitches riding on a wheel driven at 37.5 rev./min. by a synchronous motor. The time interval between the flashes was obtained from a triple exposure of a radial mark on the wheel. In order to photograph the particles, the glass end plates on the cylinder were replaced with opaque plates, one of which had a hole at the axis of the cylinder. A short black cardboard tube leading from this hole to the camera acted as a lens shade and also shielded the test region from external drafts. A triple exposure was obtained at *f*./4.5.

An enlarged section of a photograph obtained as described above is shown in Figure 3. This photograph shows clearly the groups of three images from which the velocities and streamlines were deduced. Dust tracks very near the wall were obscured by wall reflections.

The photographs were analyzed by tracing the flow lines and measuring the distance between the images of each particle. The flow lines obtained for run 4 are sketched in Figure 4. The velocities along the horizontal and vertical diameters are drawn as curved vectors, and the ends of the vectors are connected by a heavy line.

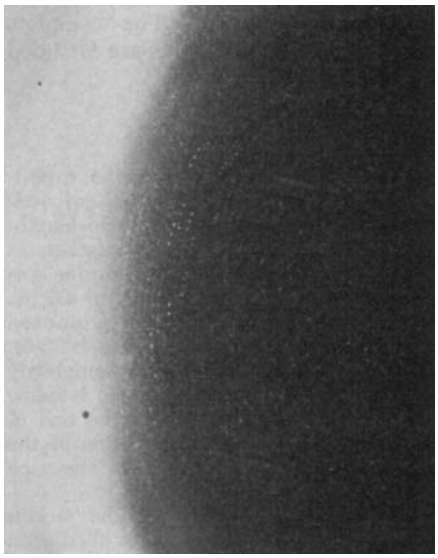

Fig. 3. Dust tracks near cold wall, run 8, T_h-T_c = 3.47°F.

FLOW FIELD

The major characteristics of the fluid motion are apparent from the streamlines and velocity vectors sketched in Figure 4 for a wall-temperature difference of 70°F. The flow patterns for all of the other experiments were quite similar. A narrow ring of gas circulates around the wall of the cylinder, but the gas in the central region is relatively stagnant. The velocity of the narrow ring of circulating gas increases up the hot wall as the gas is heated, decreases along the top of the cylinder, increases down the cold wall, and decreases again at the bottom of the cylinder. The width of the circulating ring of gas decreases up the hot wall, increases at the top, decreases down the cold side, and increases again along the bottom as required to conserve momentum. This increase and decrease in the amount of circulating gas produces large, slow eddies in the stagnant core. The motion near the wall was observed to be parallel to the wall (Figures 3 and 4), steady with time, and reproducible; therefore it can be considered laminar. The motion in the central region was also steady with time and reproducible.

Because of a positive vertical temperature gradient in the central core, the entire volume of gas does not circulate as a solid disk, as might otherwise have been expected. The central core resists rotation owing to its increasing density from top to bottom and can be considered analogous to a disk weighted at the bottom.

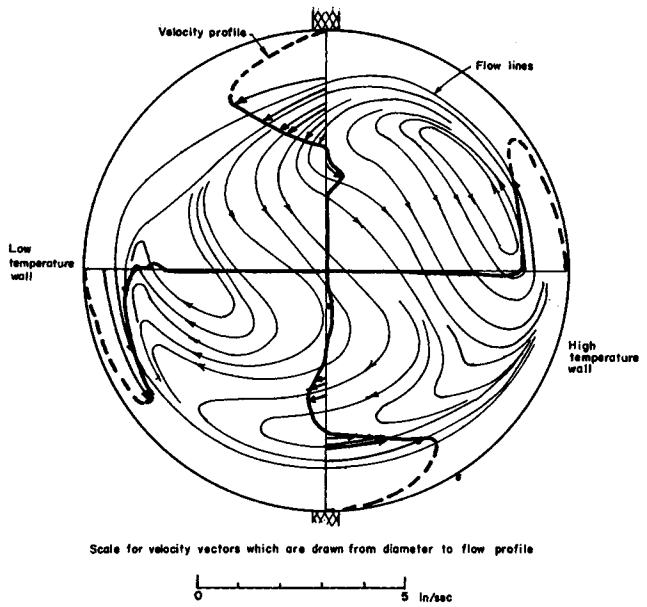

Fig. 4. Typical flow pattern, run 4, T_h-T_o = 70°F.

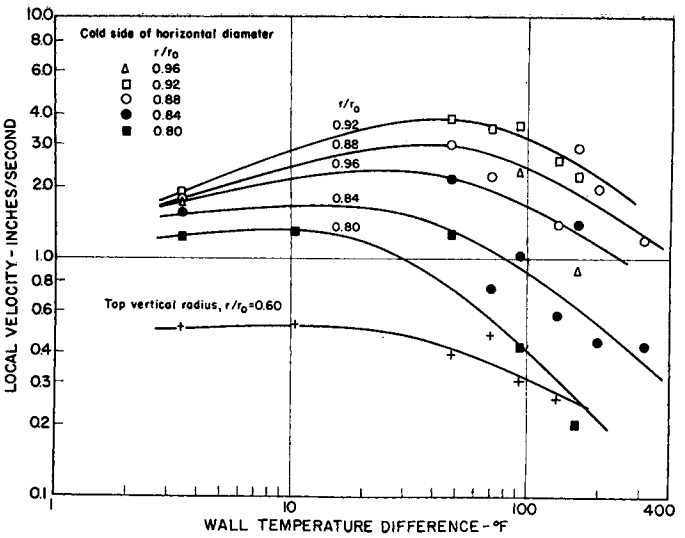

Fig. 6. Variation of local velocities with wall-temperature difference.

The velocities were determined with the most confidence along the horizontal radius on the cold side, where the illumination was most intense. Figure 5 plots the horizontal velocity profiles for three wall-temperature differences. A decrease in the width of the circulating ring with increasing wall-temperature difference can be observed. The velocities at five points along this radius and at one point in the upper vertical radius are plotted vs. wall-temperature difference in Figure 6. The data show considerable scatter but indicate a maximum velocity at all points at a wall-temperature difference of approximately 40°F.

The total volumetric and mass rates of flow across the horizontal radius on the cold side were obtained by integration, with the three velocity and temperature profiles shown in Figure 5. The maximum velocities and hence the integrated flow rates were less certain in the other runs. The results are plotted vs. temperature difference in Figure 7, indicating a rapid increase and then a slow decrease in the overall rate of circulation of gas with increasing wall-temperature difference.

TEMPERATURE FIELD

A typical set of temperature traverses is shown in Figures 8 and 9. Temperatures along the horizontal radius on the cold side are shown in Figure 5 for the same three wall-temperature differences for which the local velocities are plotted. The complete temperature data for thirteen different runs are given in reference 5. The temperature data for all thirteen runs are interpreted in the following paragraphs in terms of the local rates of heat transfer along the cylinder wall.

HEAT TRANSFER RATES

The local rate of heat transfer to or from an isothermal wall can be expressed in terms of the temperature gradient in the fluid: that is

$$\frac{dq}{dA} = -k\left(\frac{\partial T}{\partial r}\right)_{r=r_o} \qquad (1)$$

As indicated in Figure 2, the air temperature was measured along a series of horizontal and vertical lines rather than along radii only. Therefore $\partial T/\partial r$ is not directly obtainable except along the vertical and horizontal radii. However as an approximation

$$\left(\frac{\partial T}{\partial r}\right)_{r=r_o} = -\frac{1}{\cos\phi}\left(\frac{\partial T}{\partial w}\right)_{w=0} \qquad (2)$$

This approximation was used to estimate the local rates of heat transfer from the measured temperatures.

The temperatures along the horizontal and vertical traverses were observed to vary linearly with distance near the wall. Hence the gradient was determined by fitting a straight line through three to five points near the wall by least squares. The local rate, the local heat transfer coefficient based on the wall temperature difference

$$h = \left(\frac{dq}{dA}\right)\left(\frac{1}{T_h - T_c}\right) \qquad (3)$$

and hD/k were then calculated from the gradients. The 50% confidence limits for these quantities were calculated by the method described in Duncan (7). The physical properties of the air were in all cases evaluated at the wall temperature with the values given in Eckert (8). The results are illustrated in Figure 10 for the set of data in Figures 8 and 9.

The local rates at each of the twelve positions around the wall were plotted vs. wall-temperature difference and smoothed as illustrated in Figure 11 for the horizontal radius on the cold side. The smoothed data for all positions and

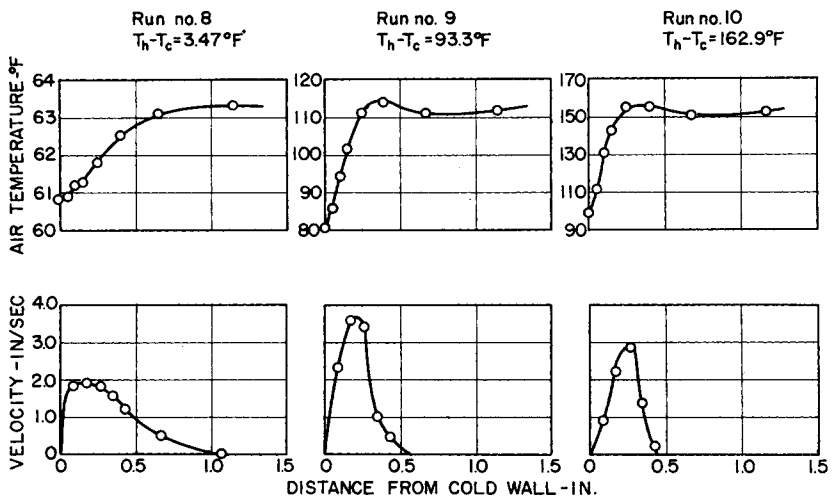

Fig. 5. Velocity and temperature distribution along horizontal radius on cold side.

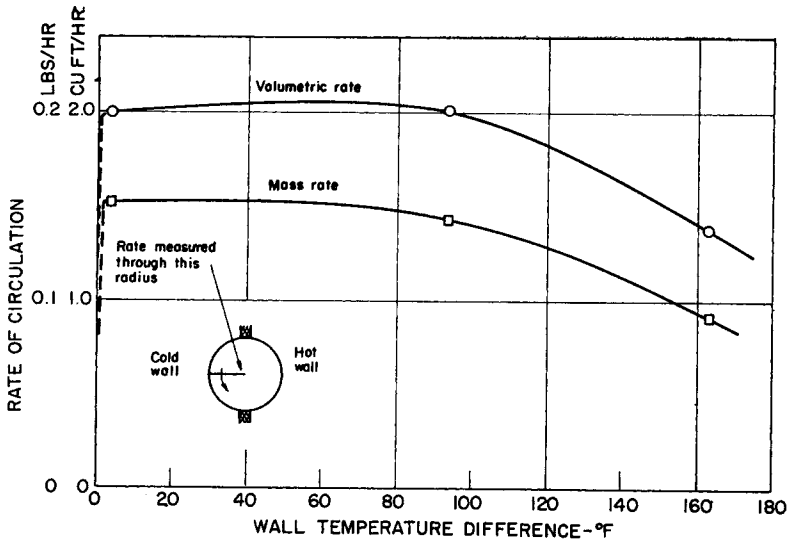

Fig. 7. Boundary-layer circulation through horizontal radius on cold side.

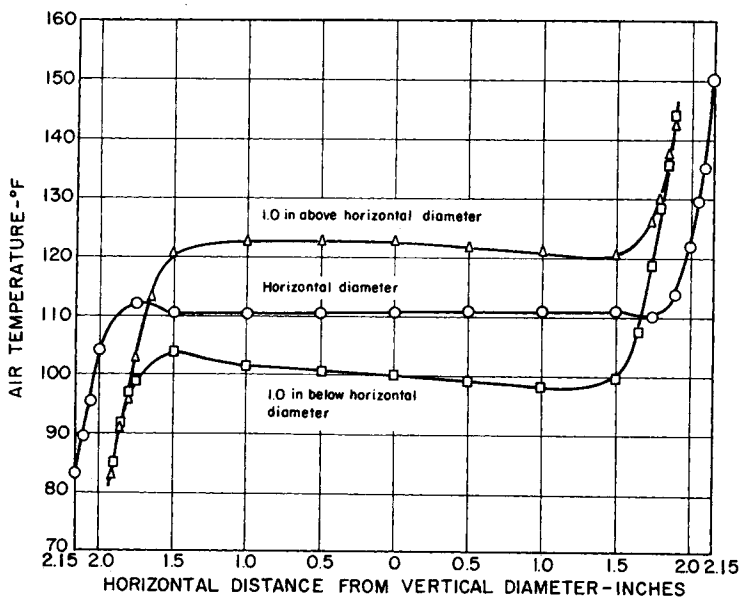

Fig. 8. Horizontal temperature profiles, run 4, T_h-T_c = 70°F.

temperature differences are summarized in Figure 12. Since the temperature and velocity fields were not symmetrical on the hot and cold sides, symmetry in the heat transfer rates was not to be expected.

The over-all rates of heat transfer were determined by graphical integration of the local rates. For example the areas above the curve on the right and below the curve on the left in Figure 10 are divided by 180° to obtain the corresponding over-all Nusselt number h_mD/k for the heated side and cooled sides, respectively. The over-all rates, heat transfer coefficients, and Nusselt numbers determined from these integrations are given in Table 1. Owing to significant heat losses through the insulation to the surroundings and owing to radiation from the hot wall to the cold, the data obtained from the wattmeter and the cooling water stream do not provide direct information on the rate of heat transfer by convection. Accordingly these data are not reproduced herein.

TABLE 1. OVER-ALL HEAT TRANSFER RATE DATA

Run	T_h, °F.	T_c, °F.	T_h-T_c, °F.	$\left[\frac{C_p\mu}{k}\right]\left[\frac{gD^3\beta(T_h-T_c)}{\nu^2}\right]10^{-6}$ Cold side	Hot side	h_m, B.t.u./(hr.)(sq. ft.)(°F.) Cold side	Hot side	h_mD/k Cold side	Hot side
3	149.9	106.7	43.2	2.21	1.572	0.266	0.362	6.03	7.47
4	146.1	76.1	70.0	4.58	2.62	0.328	0.411	7.82	8.74
5	108.0	61.7	46.3	3.43	2.34	0.244	0.303	5.92	6.83
6	104.4	67.1	37.3	2.66	1.954	0.224	0.270	5.42	6.13
7	73.1	62.8	10.3	0.760	0.697	0.147	0.165	3.57	3.95
8	64.63	61.16	3.47	0.258	0.250	0.249	0.283	6.07	6.85
9	162.4	69.1	93.3	6.52	3.07	0.218	0.340	5.25	7.06
10	241.9	79.0	162.9	10.44	2.64	0.332	0.449	7.87	8.13
11	212.4	77.0	135.4	8.83	3.13	0.303	0.434	7.20	8.41
12	297.1	98.2	198.9	10.90	1.868	0.253	0.439	5.79	7.04
13	296.1	95.9	200.2	11.16	1.898	0.266	0.573	5.93	7.26
14	428.5	115.1	313.4	15.09	1.052	0.274	0.637	6.09	7.32
15	489.4	122.8	366.6	16.29	0.837	0.261	0.456	6.03	7.33

The over-all rates determined from the temperature field are plotted in Figure 13 as heat transfer coefficients vs. temperature difference. The coefficients show only a slight increase as the temperature difference increases from 3.5° to 367°F. Curves representing the correlations of Griffiths and Davis (*9*); Jakob (*6*); and Peck, Fagan, and Werlein (*10*) for natural convection in air between enclosed vertical plates are included in Figure 13. The observed coefficients for the cylindrical region are of the same order of magnitude. Since these three previous correlations represent data taken in rectangular regions where the height was at least three times the width, and since the data are not compared in dimensionless form, this agreement is rather surprising and perhaps coincidental.

The experimental data for heat transfer by natural convection for other geometries and boundary conditions have been correlated successfully in terms of the dimensionless groups Nu and $Pr \cdot Gr$ only. Therefore the results of this investigation can be interpreted with some justification in this general form even though the experiments were limited to a single diameter and to air at atmospheric pressure. The over-all coefficient is plotted as $Nu = h_mD/k$ vs. $Pr \cdot Gr = (C_p\mu/k)(gD^3\beta[T_h-T_c]/\nu^2)$ in Figure 14 with all properties evaluated at the wall temperature. Although $Pr \cdot Gr$ was varied over two orders of magnitude, no significant trend in Nu is apparent. The experimental values of h_mD/k have a mean value of approximately 7.0.

The data in Figures 6, 7, and 11 might similarly be reinterpreted in dimensionless terms.

MACHINE COMPUTATIONS

Numerical solution of the simultaneous partial differential equations describing conservation of mass, energy, and momentum in a gas inside an in-

finite horizontal cylinder with a vertical step in wall temperature was attempted on an IBM-650 magnetic drum computer. The details of this computational experience are presented in reference 5, and only the more significant features are reported herein.

The region within the cylinder was divided into a grid of points representing elemental volumes, and the differential equations were approximated by finite difference equations in terms of the temperatures and velocities at these points. The resulting set of algebraic equations was then solved by reiteration in real time, yielding an unsteady state solution with the steady state solution as an asymptote.

Because of storage limitations of the computer, an explicit representation was used; that is the spatial derivatives of temperature and velocity were written in terms of present and incrementally past values of the variables. Extensive exploratory calculations indicated that the explicit representation was unstable for any time increment. Solution of the mass and momentum equations only, with fixed values for the temperature field from the experimental measurements, was also unsuccessful owing to instability.

A convergent solution for the energy equations only was obtained by the use of fixed values for the velocity field taken from the experimental measurements. The computed dimensionless isotherms for conditions equivalent to run 4 are compared with the experimental values in Figure 15. Significant uncertainties in the measured velocities, as well as idealizations in the differential representation, the finite number of grid points, round-off errors, and failure to carry the computations completely to the steady state could be expected to introduce discrepancies between the experimental and computed temperatures. In view of these considerations the agreement is quite reasonable. The most apparent discrepancy in the temperature is the 20-deg. inclination of the computed isotherms toward the hot side in the central region as compared with the almost horizontal measured isotherms.

The temperature gradients at the wall which determine the rate of heat transfer are compared in Figure 16. This is a very critical test in which errors are magnified by an order of magnitude, and the agreement is surprisingly good. The saw-tooth behavior in the computed curve occurs because alternate points rather than consecutive points are associated in the computations. The construction of a smooth curve between the points would therefore have been justifiable if the objective were to produce the best estimate of the gradient rather than to illustrate the results obtained by computation. If the thermal conductivity were constant, the net area under the curve should be zero, since as much heat must leave the gas as enters. The experimental gradient integrates to very nearly zero, but the computed gradient shows a net heat input.

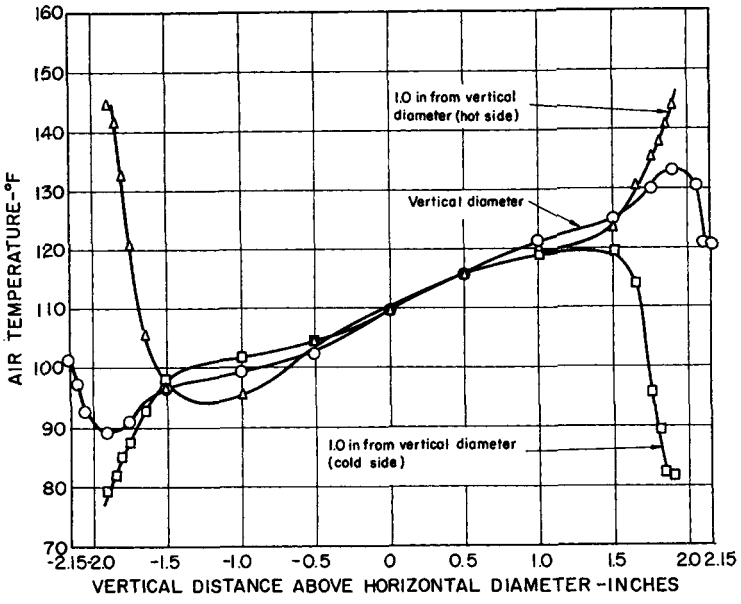

Fig. 9. Vertical temperature profiles, run 4, T_h-T_c = 70°F.

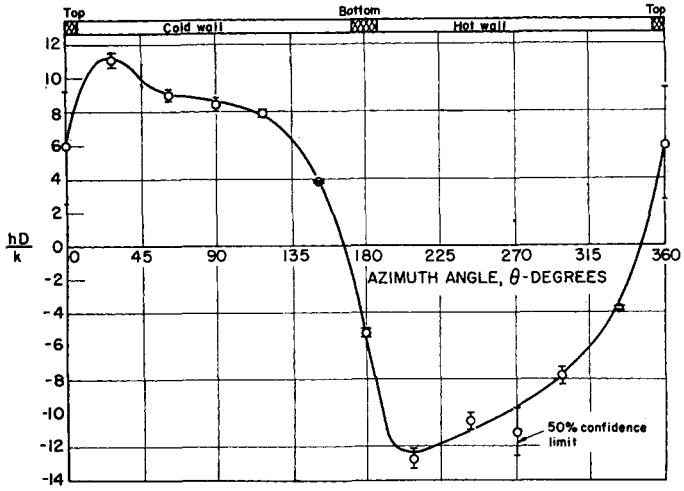

Fig. 10. Local Nusselt number, run 4, T_h-T_c = 70°F.

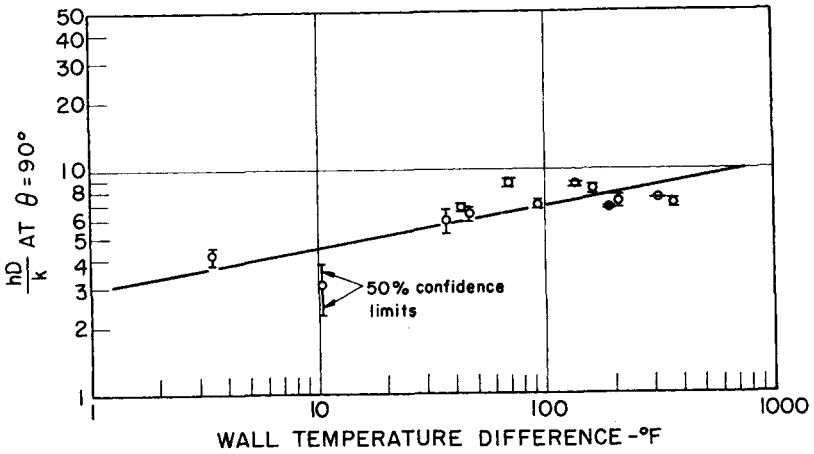

Fig. 11. Example of smoothing of local Nusselt number.

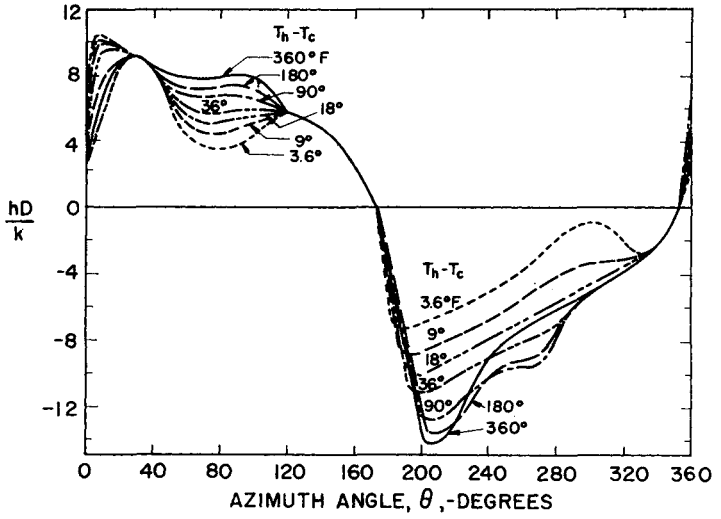

Fig. 12. Smoothed correlation for local Nusselt number.

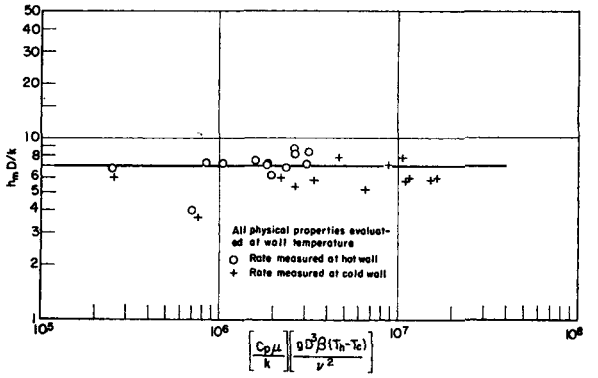

Fig. 14. Generalized correlation for natural convection inside a horizontal cylinder.

This success with the energy equation and the failure with the momentum and mass equations suggests that the nonlinearity of the momentum equations is the key to the instability of the general problem. Linearization of the momentum equations by some transformation or idealization would undoubtedly yield stable difference equations. However such a procedure loses the very advantages of exactness promised by numerical integration. A stable procedure probably can be developed with implicit representations, but such a program is feasible only on a computer with much greater storage than the IBM-650.

CONCLUSIONS

Although the experimental investigation was exploratory rather than definitive, several general conclusions can be drawn concerning the fluid motion and the rate of heat transfer in a circular cylinder with a vertical step function in wall temperature:

1. The air circulates rapidly in a narrow band near the wall while the central core of air is essentially stagnant.
2. The circulation rate increases rapidly and then decreases slowly with increasing wall-temperature difference.
3. The local heat transfer coefficient varies considerably with angle and increases only slightly with increasing wall-temperature difference.
4. The over-all rate of heat transfer by convection for air at atmospheric pressure inside a 4.3-in. cylinder corresponds to a coefficient of approximately 0.3 B.t.u./(hr.)(sq. ft.)(°F.) or a Nusselt number of approximately 7 over a range of wall-temperature difference from 3.5° to 367°F.

Several general conclusions can similarly be drawn from the exploratory computational investigation:

1. Explicit finite difference representations for the momentum, energy, and mass equations appear to be unstable for any size of the time increment.
2. The instability is apparently due to the nonlinear terms in the momentum equation.
3. A stable procedure probably can be developed with implicit representations, but such a program requires a computer with greater storage than the IBM-650.
4. The agreement demonstrated between the measured temperatures and those computed by utilizing the measured velocities gives support to both the experimental values and to the numerical representation and computational procedure.
5. A method for a priori machine computation of natural convection for any boundary conditions and physical properties has real economic as well as scientific value. This computational experience is believed to be a significant step in developing such a method even though only partial success was realized.

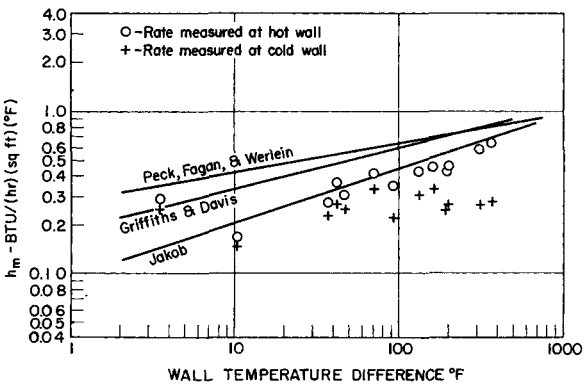

Fig. 13. Comparison of experimental correlations for natural convection.

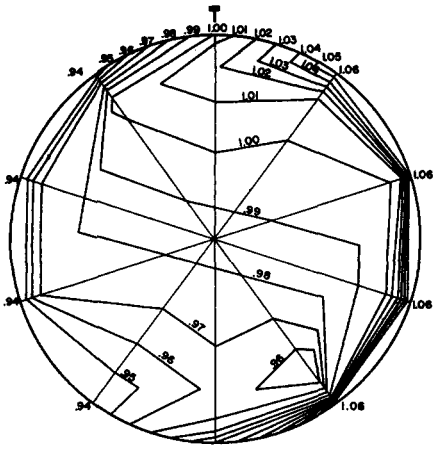

a Calculated

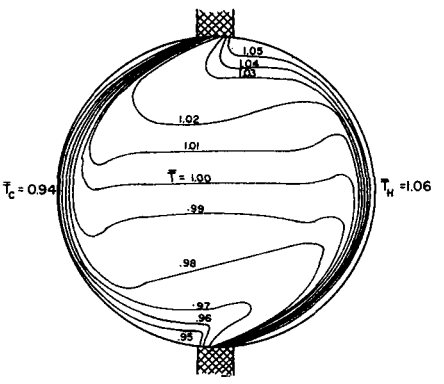

b Experimental

Fig. 15. Comparison of computed and measured isotherms, run 4, $T_h - T_o = 70°F$.

NOTATION

A = surface area, sq. ft.
C_p = heat capacity, B.t.u./(lb.)(°F.)
D = diameter of cylinder, ft.
g = acceleration due to gravity, (ft./hr.)/hr.
Gr = $gD^3\beta(t_h-T_c)/\nu^2$ = Grashof number
h = local heat transfer coefficient based on wall-temperature difference, B.t.u./(hr.)(sq. ft.)(°F.)
h_m = mean heat transfer coefficient over cold or hot wall based on wall-temperature difference, B.t.u./(hr.)(sq. ft.)(°F.)
k = thermal conductivity of gas, B.t.u./(hr.)(sq. ft.)(°F./ft.)
Nu = h_mD/k = Nusselt number
Pr = $C_p\mu/k$ = Prandtl number
q = heat flux to wall, B.t.u./hr.
r = radial distance from axis of cylinder, ft.
r_o = radius of cylinder, ft.
$\overline{r}$ = r/D = dimensionless radial distance
T = temperature, °R.
T_c = temperature of cold wall, °R.
T_h = temperature of hot wall, °R.
T_o = $(T_h+T_c)/2$ = reference temperature, °R.
$\overline{T}$ = T/T_o = dimensionless temperature

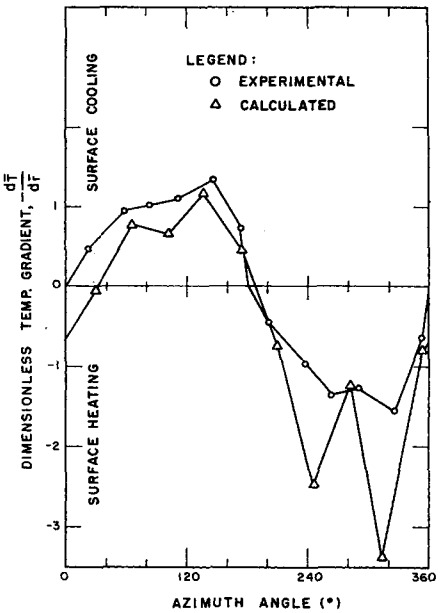

Fig. 16. Comparison of computed and measured temperature gradients, run 4, T_h-T_o = 70°F.

w = distance from wall along a temperature traverse, ft.

Greek Letters

β = volumetric coefficient of expansion, $°R^{-1}$
θ = azimuth angle from top of cylinder through cold side, deg.
μ = viscosity, lb./(ft.)(hr.)
ν = kinematic viscosity, (sq. ft.)/hr.
ϕ = angle between traverse line and radial line at cylinder wall, deg.

LITERATURE CITED

1. Ostroumov, G. A., *Doklady Akad. Nauk S.S.S.R.*, **71**, 887 (1950)
2. Zhukhovitskii, E. M., *Zhur. Tekh. Fiz.*, **22**, 832 (1952).
3. Drakhlin, E., *ibid.*, **22**, 829 (1952).
4. Shaposhnikov, I. G., *ibid.*, **22**, 826 (1952).
5. Martini, W. R., Ph.D. thesis, Univ. Michigan, Ann Arbor (1956).
6. Jakob, Max, "Heat Transfer," vol. I., John Wiley, New York (1949).
7. Duncan, A. J., "Quality Control and Industrial Statistics," Richard D. Irvin, Inc., Homewood, Ill. (1953).
8. Eckert, E. R. G., "Introduction to the Transfer of Heat and Mass," McGraw-Hill, New York (1950).
9. Griffiths, E., and A. H. Davis, "The Transmission of Heat by Radiation and Convection," Food Investigation Board Special Report No. 9, His Majesty's Stationary Office, London, England (1922).
10. Peck, R. E., W. S. Fagan, and P. P. Werlein, *Trans. Am. Soc. Mech. Engrs.*, **73**, 281 (1951).

Manuscript received May 1, 1957; revision received September 10, 1959; paper accepted October 12, 1959. Material presented at 1957 Nuclear Congress and A.I.Ch.E. Atlantic City meeting.

The Compressibility of Carbon Dioxide-Argon Mixtures

WILLIAM H. ABRAHAM and C. O. BENNETT

Purdue University, Lafayette, Indiana

The compressibility factor has been measured at 50°C. and 50 to 1,000 atm. for each of seven mixtures of carbon dioxide and argon containing 12.9 to 83.1 mole % carbon dioxide. The compressibility factors are reported as smoothed values at even pressures and also in the form of empirical smoothing expressions which fit the experimental values with an average absolute deviation of 0.1%. Various methods of predicting gas-mixture compressibility are tested, and activity coefficients calculated from the experimental data are reported.

Despite more than 200 previous high-pressure P-V-T studies (5), it is still not possible to predict accurately the compressibility at high pressures of a gas for which experimental compressibility data are not available. The best methods of predicting gas-mixture compressibilities, for example, may be in error by 5% at only a few hundred atmospheres of pressure. As a corollary the prediction of properties derived from the compressibility, such as the fugacity of the component of a gaseous mixture, is still more uncertain.

The present experimental study of the compressibility of mixtures of carbon dioxide and argon provides new information about gas-mixture compressibility at temperatures and pressures approaching the critical region, where previous experimental information is rather limited. Seven different mixtures of carbon dioxide and argon were investigated, at 50°C. and pressures of 50 to 1,000 atm. The use of a large number of mixtures permits the calculation of accurate values of the fugacity of the components of the mixture.

William H. Abraham is with E. I. du Pont de Nemours, Inc., Wilmington, Delaware. C. O. Bennett is with the Lummus Company, New York, New York.